Am J Physiol Heart Circ Physiol 305: H1658–H1667, 2013.
First published September 16, 2013; doi:10.1152/ajpheart.00349.2013.

A novel heart failure mice model of hypertensive heart disease by angiotensin II infusion, nephrectomy, and salt loading

Yasumasa Tsukamoto,[1,2] Toshiaki Mano,[1,2] Yasushi Sakata,[1] Tomohito Ohtani,[1] Yasuharu Takeda,[1] Shunsuke Tamaki,[1,2] Yosuke Omori,[1,2] Yukitoshi Ikeya,[1,3] Yuki Saito,[1,3] Ryohei Ishii,[4] Mitsuru Higashimori,[4] Makoto Kaneko,[4] Takeshi Miwa,[2] Kazuhiro Yamamoto,[5] and Issei Komuro[1]

[1]*Department of Cardiovascular Medicine, Osaka University Graduate School of Medicine, Suita, Japan;* [2]*Genome Information Research Center, Osaka University, Suita, Japan;* [3]*Division of Cardiology, Department of Internal Medicine, Nihon University School of Medicine, Tokyo, Japan;* [4]*Department of Mechanical Engineering, Osaka University, Suita, Japan; and* [5]*Department of Molecular Medicine and Therapeutics, Faculty of Medicine, Tottori University, Yonago, Japan*

Submitted 24 April 2013; accepted in final form 13 September 2013

Tsukamoto Y, Mano T, Sakata Y, Ohtani T, Takeda Y, Tamaki S, Omori Y, Ikeya Y, Saito Y, Ishii R, Higashimori M, Kaneko M, Miwa T, Yamamoto K, Komuro I. A novel heart failure mice model of hypertensive heart disease by angiotensin II infusion, nephrectomy, and salt loading. *Am J Physiol Heart Circ Physiol* 305: H1658–H1667, 2013. First published September 16, 2013; doi:10.1152/ajpheart.00349.2013.—Although the mouse heart failure (HF) model of hypertensive heart disease (HHD) is useful to investigate the pathophysiology and new therapeutic targets for HHD, the model using simple experimental procedures and stable phenotypes has not been established. This study aimed to develop a novel mouse HF model of HHD by combining salt loading and uninephrectomy with ANG II infusion. Eight-week-old C57BL/6 male mice were treated with ANG II infusion (AT), ANG II infusion and uninephrectomy (AN), ANG II infusion and salt loading (AS), or ANG II infusion, uninephrectomy, and salt loading (ANS). Systolic blood pressure was significantly elevated and left ventricular (LV) hypertrophy was found in AT, AN, AS, and ANS mice, and there were no significant differences in those parameters between the four groups. At 6 wk after the procedures, only ANS mice showed significant decreases in LV fractional shortening and increases in lung weight with a high incidence. This phenotype was reproducible, and there were few perioperative or early deaths in the experimental procedures. Severe LV fibrosis was found in ANS mice. Oxidative stress was enhanced and small GTPase Rac1 activity was upregulated in the hearts of ANS mice. After the addition of salt loading and uninephrectomy to the ANG II infusion mouse model, cardiac function was significantly impaired, and mice developed HF. This might be a novel and useful mouse HF model to study the transition from compensated LV hypertrophy to HF in HHD.

heart failure; mouse model; angiotensin II; renal dysfunction; salt loading; hypertensive heart disease

HYPERTENSIVE HEART DISEASE (HHD) is a major public health problem that contributes to cardiovascular morbidity and mortality. HHD patients with persistent pressure overload often demonstrate a transition from a phase of compensated hypertrophy to heart failure (HF). However, the mechanism of this transition is still unclear.

Animal models of HF have contributed greatly to the development of novel HF therapies or the elucidation of pathophysiology of HHD. Several animal models that mimic features of HHD have been used over the years (15). Large animal or rat models, such as the renal wrap dog model (11), spontaneously hypertensive rat (36), and Dahl salt-sensitive rat (4), have been generally used as models of HHD. Mice with genetic modification are valuable tools to study the mechanisms of various cardiovascular diseases. The C57BL/6 mouse strain serves as the genetic background of many transgenic and gene knockout models to validate the function of specific genes. Previous studies (10, 12, 49) have shown that ANG II infusion mouse models develop HHD with cardiac hypertrophy and fibrosis, but C57BL/6 mice infused with high doses of ANG II maintain cardiac function and do not develop HF (10, 12, 49). The transverse aortic constriction (TAC) model has been used for a mouse model of pressure overload (26), but it does not entirely mimic human HHD, and it is also difficult to prepare the model because microsurgical skills are required. Thus, there are few appropriate mouse models of HHD that mimic clinical HHD well and develop HF.

It is well known that chronic kidney disease (CKD) increases the risk of cardiovascular events and overall deaths (6) and is associated with HHD. It has been reported that uninephrectomy induces renal dysfunction, especially under the high-salt condition, in animal models (2, 38), although it is controversial whether uninephrectomy itself is generally a risk factor for CKD in humans (16, 47). High salt intake is also associated with the occurrence of hypertension (7) and significantly increases the risk of total cardiovascular disease (44).

In the present study, we sought to establish a new model of HHD in C57BL/6 mice by combining salt loading, uninephrectomy, and chronic ANG II infusion.

METHODS

This study conformed with the guiding principles of and was approved by Osaka University Graduate School of Medicine with regard to animal care and conformed with the National Institutes of Health (NIH) *Guide for the Care and Use of Laboratory Animals*.

Animal procedures. The procedures used for the different groups are shown in Table 1. Eight-week-old male C57BL/6 mice (Japan SLC, Shizuoka, Japan) were anesthetized with a mixture of ketamine HCl (80 mg/kg ip) and xylazine HCl (10 mg/kg ip). Mice were divided into the following groups: control, ANG II infusion (AT group), ANG II infusion and uninephrectomy (AN group), ANG II infusion and salt loading (AS group), and ANG II infusion, uninephrectomy, and salt loading (ANS group). The left kidneys of ANS and AN mice were removed through a flank incision (uninephrectomy). Control, AT, and AS mice underwent sham surgery by exposing the left kidney without removal. AT, AN, AS, and ANS mice were infused with ANG II (1.2 mg·kg^{-1}·day^{-1}, Sigma-Aldrich) by subcu-

Address for reprint requests and other correspondence: T. Mano, Dept. of Cardiovascular Medicine, Osaka Univ. Graduate School of Medicine, 2-2 Yamadaoka, Suita 565-0871, Japan (e-mail: mano@medone.med.osaka-u.ac.jp).

Table 1. *Procedures of the mouse model*

	Control Group	AT Group	AN Group	AS Group	ANS Group
ANG II infusion	−	+	+	+	+
Uninephrectomy	−	−	+	−	+
Salt loading (1% NaCl in drinking water)	−	−	−	+	+

Mice were divided into the following groups: control, ANG II infusion (AT group), ANG II infusion and uninephrectomy (AN group), ANG II infusion and salt loading (AS group), and ANG II infusion, uninephrectomy, and salt loading (ANS group).

taneous implantation of an osmotic minipump (Alza) immediately after the uninephrectomy/sham procedure. ANG II was dissolved in 0.01 mol/l acetic acid-saline. Osmotic minipumps containing 0.01 mol/l acetic acid-saline were implanted in control mice. After the procedures, AS and ANS mice were given drinking water containing 1% NaCl. All mice were fed a normal salt diet (rodent chow containing 0.3% NaCl). The diet and tap water were provided ad libitum throughout the experiment.

After the surgery, conscious systolic blood pressure (SBP) was monitored weekly with a tail-cuff system (BP-98A, Softron, Tokyo, Japan). Mice were analyzed 6 wk after surgery.

Echocardiography in mice. For the evaluation of cardiac dimension and contractility, a transthoracic echocardiographic experiment was performed on conscious mice using an echocardiographic machine equipped with a 25-MHz linear probe (Vevo 770, Visual Sonics), as previously described (25).

Tissue and blood sampling in mice. After echocardiography, mice were anesthetized with an intraperitoneal injection of ketamine and xylazine (100 and 10 mg/kg, respectively). Blood was collected from the inferior vena cava. The serum creatinine concentration was measured by an enzymatic method (21). The heart and lung were rapidly harvested, and the left ventricle (LV) and lung were weighed. LV and lung weight were corrected for tibial length. The apical part of the LV myocardium was snap frozen in liquid nitrogen and stored at −80°C for 2 wk before measurement of mRNA and Rac1 activities. Samples for immunohistochemistry were embedded in Tissue-Tek OCT compound (Sakura Finetechnical, Tokyo, Japan) and frozen. The rest of the LV and lung samples were fixed with phosphate-buffered 10% formalin solution for 48 h. Specimens were embedded in paraffin for histological analyses, 2-μm-thick sections of the lungs were stained with hematoxylin and eosin for routine histological examination, and 2 μm-thick transverse sections of the LV were stained with Sirius red for the detection of fibrosis (33). A whole LV transverse section image was made of 30–40 color ×100 magnification images using a digital microscopy and software (BZ-8000, Keyence, Osaka, Japan), and the ratio of the interstitial fibrosis area to myocardial area in a whole LV section was calculated. Fibrosis of the perivascular, epicardial, and endocardial areas was excluded from the analysis. TRITC-labeled lectin from *Triticum vulgaris* (Sigma) was used for membrane staining (31). Sections were analyzed with fluorescent digital microscopy (BZ-8000, Keyence). Suitable cross-sections of cardiomyocytes for the area measurements were defined as having round to oval membrane staining from which the area was calculated. The fibrosis area, myocardial area, and cross-sectional area of cardiomyocytes were measured using NIH ImageJ 1.43u software.

Hemodynamic analysis. Mice that survived over 35 days after surgery were assessed for open-chest approach hemodynamic measurements as previously described (13, 34, 45). Anesthesia was induced with 3% followed by 1.5% isoflurane once the mice were intubated. The adequacy of anesthesia was monitored by the stability of blood pressure, heart rate, and lack of flexor responses to a paw pinch. A Millar 1.0-Fr high-fidelity manometer-tipped catheter (SPR-1000) was inserted into the LV after a stab of the apex with a 26-gauge needle through the stab wound to record LV pressure to determine the LV end-diastolic pressure (LVEDP), peak positive rate of LV pressure development (+dP/dt), and time constant of LV relaxation (τ).

Measurement of LV myocardial stiffness in mice. We evaluated LV myocardial stiffness at 4 wk after surgery with a balloon-type sensing system as previously described (17, 45). Skinned LV muscles from mice were prepared according to previously reported methods (46). The skinned transverse section was placed around a latex balloon (Labo Support) while the pressure inside the balloon was monitored. The balloon was then dilated with the deformation information of the balloon and the specimen captured by a charge-coupled device camera. Young's modulus (E_H) was obtained from the internal pressure of the balloon and the strain of the transverse LV section based on a dual-cylinder model.

Measurements of mRNA levels. Total RNA was extracted from LV tissue and reverse transcribed to cDNA as previously described (50). Quantitative real-time RT-PCR with the ABI PRISM 7900 HT Sequence Detection System and software (Applied Biosystems, Foster City, CA) was conducted to measure mRNA levels of β-actin, atrial natriuretic peptide (ANP), brain natriuretic peptide (BNP), collagen type Iα, and connective tissue growth factor (CTGF). The sequence of the primers and Taqman probes for BNP and CTGF have been previously described (5, 19). The primers and Taqman probes for β-actin, ANP, and collagen type Iα were assays-on-demand gene expression products (assay identifiers: Mm00607939_s1, Mm01255748_g1, and Mm00801666_g1, respectively, Applied Biosystems). The amount of each mRNA was divided by β-actin mRNA to correct the efficiency of cDNA synthesis and normalized to the mean of the control.

Immunohistochemistry for 4-hydroxy-2-nonenal protein expression. The expression of 4-hydroxy-2-nonenal (4-HNE), a byproduct of lipid peroxidation and an indicator for oxidative stress, was determined by immunohistochemical staining. Cryostat transverse sections were stained with mouse monoclonal anti-4-HNE antibody (1:50 dilution, NOF Medical Department, Tokyo, Japan) as previously described (30) using the mouse on mouse system (Nichirei Bioscience, Tokyo, Japan). The area and intensity of staining for HNE were blinded to the score for semiquantification (32). The scoring range was defined as as follows: *0* = no visible staining, *1* = faint staining, *2* = moderate staining, *3* = strong staining, and *4* = very strong staining. Scores were determined by three independent observers blinded for the identification of the mice and were averaged.

In vitro experiments in cultured cardiomyocytes. Neonatal rat cardiac ventricular myocytes were isolated using standard techniques from Wistar rats with modifications of previously described methods (9, 29). Cardiomyocytes were suspended in 50% DMEM (Invitrogen) plus 50% medium 199 (M199; Invitrogen) supplemented with 10% FCS (Invitrogen). Cells were allowed to attach for 24 h. The medium was replaced with serum-free 50% DMEM plus 50% M199 (referred to as "control medium"), and cells were incubated for an additional 24 h. To assess the effects of high salt and ANG II, cardiomyocytes were incubated with high-salt medium (Na^+ concentration of 162 mmol/l) or ANG II (1 μmol/l, Sigma) for 3 h. The high-salt medium was made by simply adding NaCl. Cardiomyocytes with control medium (Na^+ concentration of 150 mmol/l) were used as controls. Cellular protein content was quantified by a modified Lowry assay.

Measurement of Rac1 activities. Activated Rac1 was analyzed by the p21-binding domain of a p21-activated protein kinase 1 pulldown assay with a commercially available kit (Rac1 Activation Assay Kit, Cell Biolabs, San Diego, CA) according to the manufacturer's protocol (41).

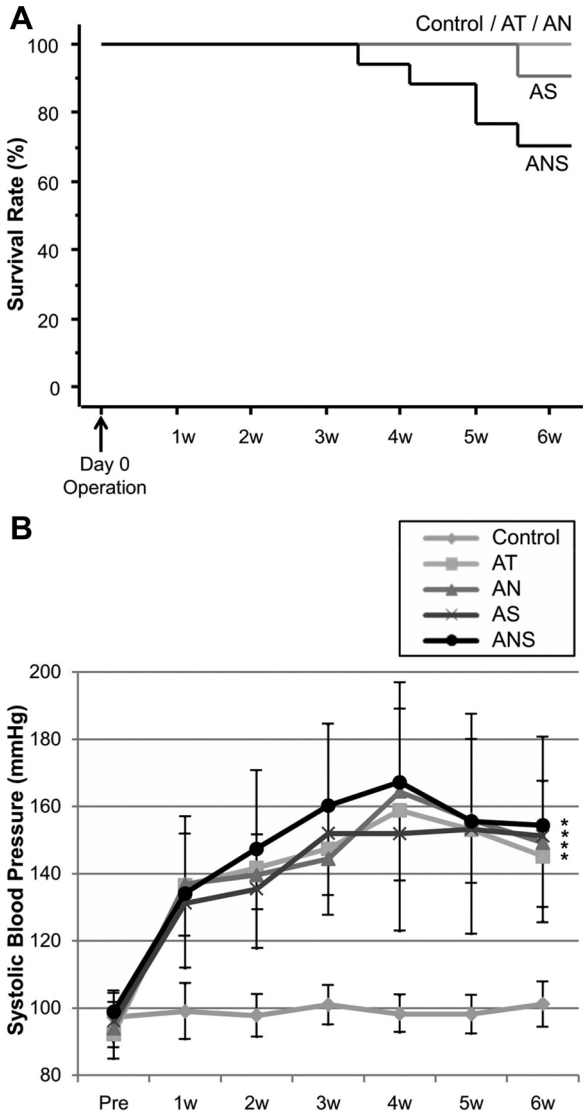

Fig. 1. Survival curves and systolic blood pressure (SBP) in the mouse model. *A*: survival curves of control, ANG II infusion (AT), ANG II infusion and uninephrectomy (AN), ANG II infusion and salt loading (AS), and ANG II infusion, uninephrectomy, and salt loading (ANS) mouse groups after the procedures. *B*: SBP values of the five groups over the time course of the experiment. Values are means ± SD. *$P < 0.05$ vs. the control group.

Statistical analysis. Data are presented as means ± SD and were analyzed using statistical software (STATVIEW version 5.0, SAS Institute, Cary, NC). Multiple-group comparison was performed by one-way ANOVA followed by the Tukey-Kramer method for comparison of means. The time course of SBP among multiple groups was assessed using repeated-measures ANOVA followed by the Tukey's test. Comparisons between two groups were analyzed by an unpaired *t*-test. *P* values of <0.05 were considered statistically significant.

RESULTS

Mortality in mouse models. Survival curves of mice are shown in Fig. 1*A*. Mortality rates until 6 wk after surgery in control, AT, AN, AS, and ANS mice were 0%, 0%, 0%, 9.1%, and 35.3%, respectively. Significant LV dilatation and increases of lung weight were observed in all dead AS and ANS mice at necropsies. ANS mice demonstrated high mortality, which could be attributed to HF.

Physiological parameters and renal function in mouse models. The results of physiological and biochemical parameters at 6 wk after surgery are shown in Table 2, and a time course of SBP is shown in Fig. 1*B*. AT, AN, AS, and ANS mice showed significantly higher SBPs than control mice, whereas there were no significant differences in SBP among the four groups. The serum creatinine concentration was significantly higher in AN and ANS mice than in non-nephrectomized mice. This result indicates that renal dysfunction occurred in mice with uninephrectomy and ANG II infusion. Serum Na^+ levels were higher in ANS mice than in control and AT mice.

ANS mice developed HF. At 6 wk after the operation, the increase in LV end-diastolic posterior wall thickness was found to be similar in AT, AN, AS, and ANS mice compared with control mice (Fig. 2*D*). LV weight/tibial lengh was increased in AT, AN, AS, and ANS mice compared with control mice (Fig. 3*A*). Histological examination also revealed an increase in the cross-sectional area of cardiomyocytes in AT, AN, AS, and ANS mice compared with control mice (Fig. 3*D*). These parameters indicate that hypertrophy of cardiomyocytes occurred similarly in AT, AN, AS, and ANS mice. LV endocardial fractional shortening was depressed in ANS mice compared with any other group mice at 6 wk after surgery (Fig. 2*C*). The LV end-diastolic diameter of ANS mice was enlarged compared with AT, AN, and AS mice (Fig. 2*B*). ANS mice did not show LV systolic dysfunction or overt HF at 4 wk after the operation. At 5 wk after the operation, ANS mice showed LV systolic dysfunction, and 25% of ANS mice manifested congestive HF as assessed by the increase in lung weight (Table 3). An index of LV myocardial stiffness, E_H, was increased in ANS mice at 4 wk after surgery (Fig. 4*A*). LVEDP was significantly increased and LV $+dP/dt$ was decreased at 6 wk after surgery in ANS mice compared with control mice (Fig. 4*B*). τ was prolonged in ANS mice (Fig. 4*B*). These results showed that LV systolic and diastolic function were impaired in ANS mice. Lung weights were not changed in AT, AN, and AS mice

Table 2. *Physiological and biochemical parameters at 6 wk after surgery in the mouse model*

	Control Group	AT Group	AN Group	AS Group	ANS Group
Number of mice/group	12	9	10	10	11
Body weight, g	28.1 ± 1.6	26.6 ± 1.4	25.7 ± 1.7*	25.0 ± 1.3*	24.9 ± 1.7*
Tibial length mm	18.2 ± 0.3	18.2 ± 0.2	18.2 ± 0.3	18.2 ± 0.2	18.0 ± 0.2
Systolic blood pressure, mmHg	101 ± 7	145 ± 18*	149 ± 24*	151 ± 18*	154 ± 17*
Heart rate, beats/min	678 ± 67	693 ± 58	639 ± 79	701 ± 43	710 ± 52
Serum creatinine, mg/dl	0.09 ± 0.02	0.13 ± 0.03	0.20 ± 0.06*†	0.14 ± 0.04	0.20 ± 0.05*†‡
Serum Na^+, meq/l	150 ± 2.3	150 ± 1.8	153 ± 3.6	154 ± 1.7	156 ± 4.5*†

Results are means ± SD. Biochemical parameters were analyzed from blood samples from 6–8 mice/group. *$P < 0.05$ vs. the control group; †$P < 0.05$ vs. the AT group; ‡$P < 0.05$ vs. the AS group.

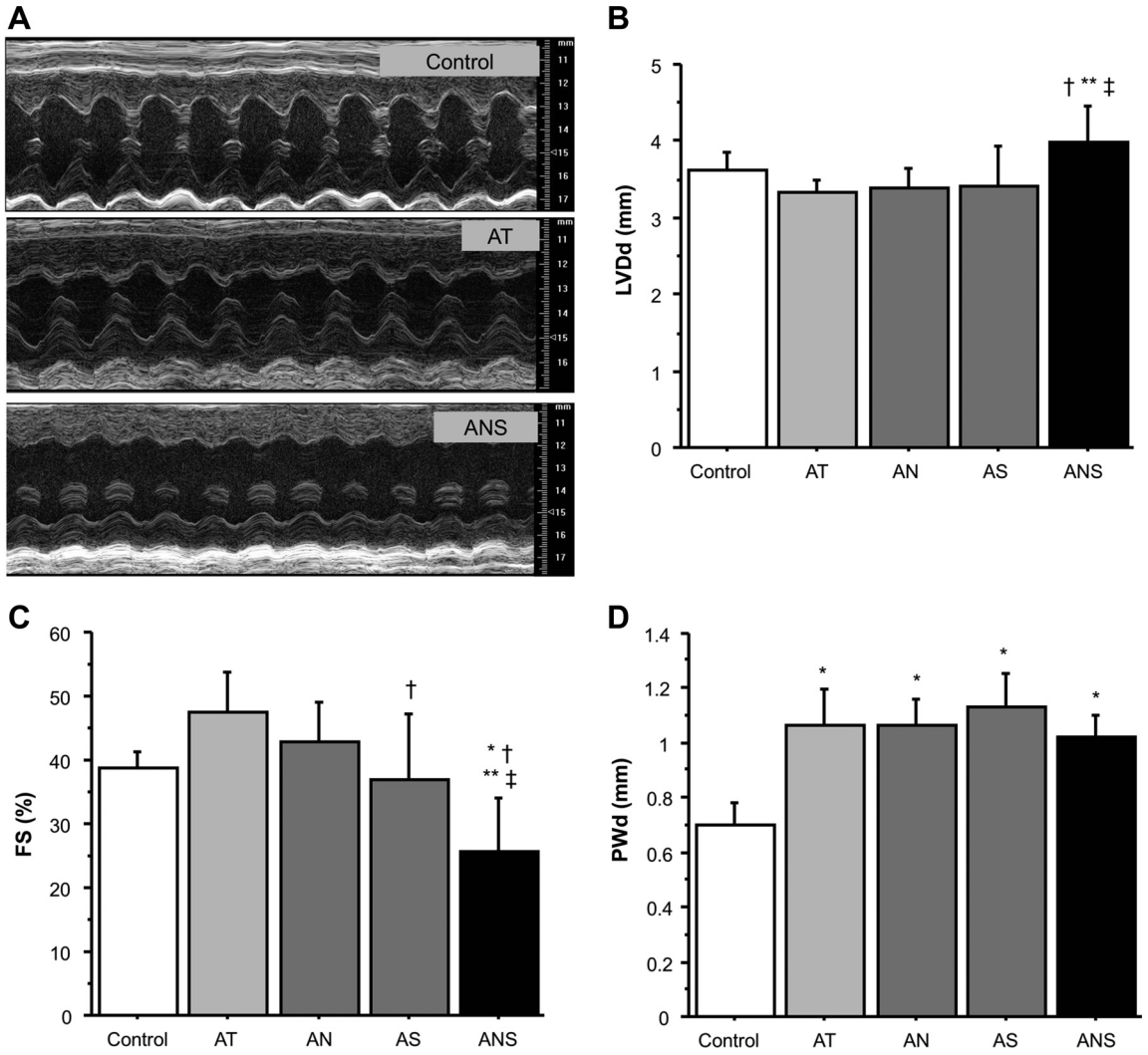

Fig. 2. Analysis with echocardiography at 6 wk after surgery in the mouse model. *A*: typical examples of M-mode echocardiograms. *B–D*: left ventricular (LV) diastolic dimension (LVDd; *B*), LV fractional shotening (FS; *C*), and end-diastolic wall thickness of the LV posterior wall (PWd; *D*) in control, AT, AN, AS, and ANS mice. *$P < 0.05$ vs. control mice; †$P < 0.05$ vs. AT mice; **$P < 0.05$ vs. AN mice; ‡$P < 0.05$ vs. AS mice.

compared with control mice, but ANS mice showed a significant increase in lung weight compared with any other group of mice. Histological observation of the lung revealed severe pulmonary alveolar edema in ANS mice. These results are consistent with pulmonary congestion. Levels of ANP and BNP mRNA expression were significantly increased in AS and ANS mice compared with control and AT mice, suggesting that additive salt loading with ANG II infusion induced an upregulation of gene expression of ANP and BNP in the LV.

Reproducibility of the phenotype of ANS mice. From three independent experiments, the reproducibility of the phenotype of ANS mice was analyzed (Table 4). LV weight increased similarly in the three experiments. This suggests that the loading condition was stable in this model of HF. The mortality rate of each experiment was 20–42%, and all of the deaths occurred between 3 and 6 wk with signs of congestive HF. Early mortality, defined as death within 2 wk after the procedures, was 0% in ANS mice. The rate of HF in the surviving mice was 67–75%, which was defined as increases in lung weights.

LV fibrosis was found in ANS mice. LV interstitial fibrosis was observed in AN, AS, and ANS mice and was severe in ANS mice (Fig. 5, *A* and B). mRNA levels of collagen type Iα were also increased in the LVs of AN, AS, and ANS mice, and ANS mice showed greater levels compared with AN mice. CTGF levels were also increased in the LVs of ANS mice compared with control, AT, and AN mice (Fig. 5, *C* and *D*).

Oxidative stress was increased in ANS mouse hearts. To examine the extent of oxidative stress in the heart, the level of 4-HNE-modified protein was assessed in cardiac tissue using immunohistochemical staining with anti-4-HNE antibody as a marker of oxidative stress. 4-HNE-modified protein adducts in the LVs of ANS mice were increased significantly compared with any other group (Fig. 6, *A* and *B*).

Rac1 activity was upregulated in ANS mouse hearts and cardiomyocytes with high salt and ANG II. Rac1 activity was significantly increased in ANS mouse hearts but not in AT, AN, or AS mouse hearts (Fig. 7*A*). Rac1 activity was significantly increased in cardiomyocytes treated with both high salt and ANG II but was not significant in cardiomyocytes with only high salt or ANG II (Fig. 7*B*).

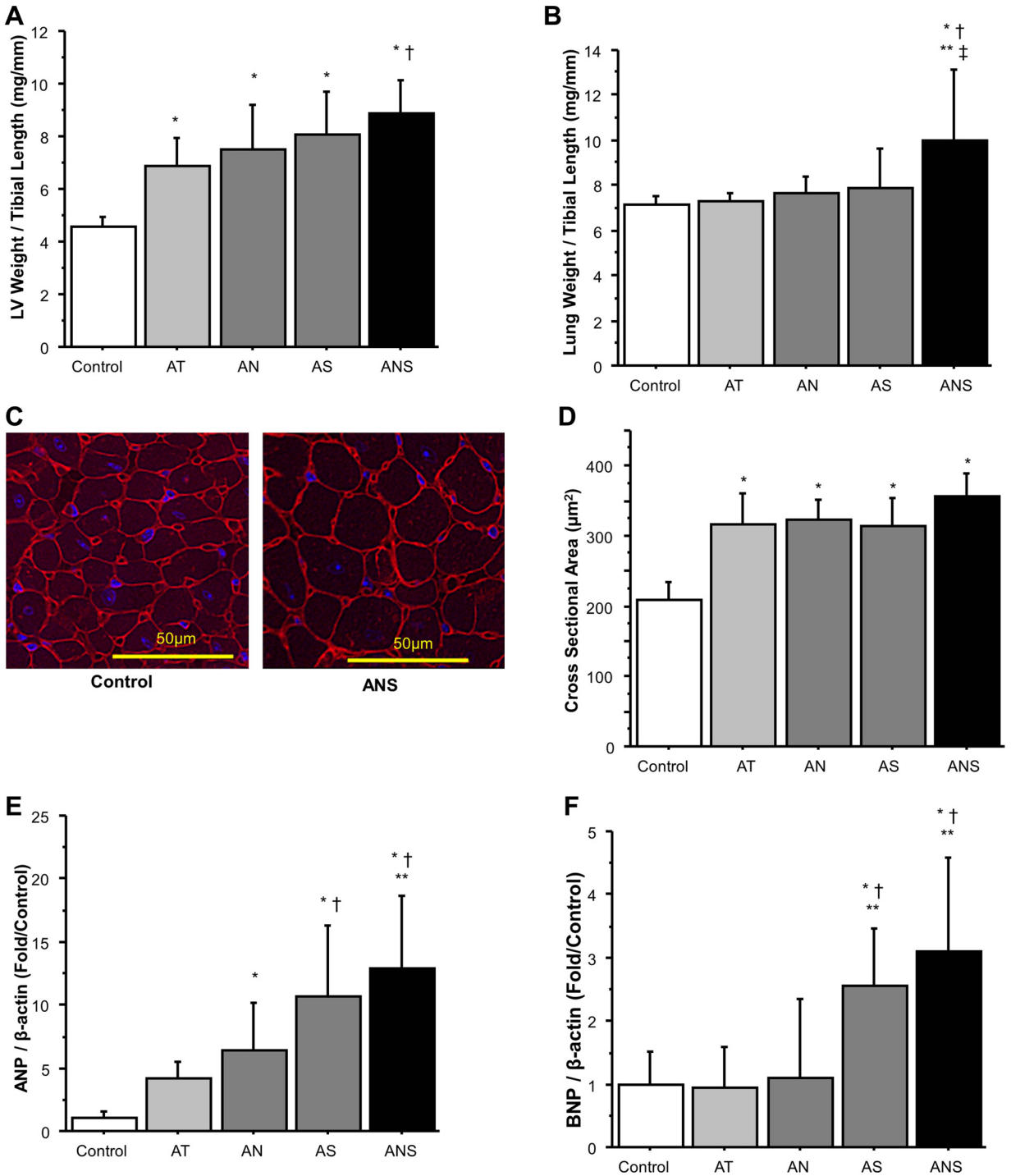

Fig. 3. Organ weights, cross-sectional areas of LV cardiomyocyte, and LV gene expression in the mouse model. *A* and *B*: LV weight/tibial length (*A*) and lung weight/tibial length (*B*) at 6 wk after surgery in control, AT, AN, AS, and ANS mice. *C*: representative examples of lectin-TRITC (red) staining of LV cross-sections. Sections were also stained for nuclei (blue). *D*: values of cross-sectional area of LV cardiomyocytes at 6 wk after the procedures in the five groups. *E* and *F*: atrial natriuretic peptide (ANP; *E*) and brain natriuretic peptide (BNP; *F*) gene expression in the LVs of the five groups. Values are means ± SD. *$P < 0.05$ vs. the control group; †$P < 0.05$ vs. the AT group; **$P < 0.05$ vs. the AN group; ‡$P < 0.05$ vs. the AS group.

DISCUSSION

The main finding of this study is that a significant decrease in LV fractional shortening with lung edema was seen after uninephrectomy, high salt intake, and ANG II infusion in this mouse model of HHD. This novel mouse model has several features that mimic clinical HHD (15). Blood pressure was elevated and LV hypertrophy developed at an early stage. Overt HF was observed with cardiac fibrosis, which is considered to be a major determinant of LV dysfunction in HHD (37) at the late stage in this model. ANG II activation is thought to induce hypertension and cardiac hypertrophy, and it also provoked cardiac fibrosis (37). Local activation of the renin-ANG

Table 3. *Physiological parameters of control and ANS mice from 4–6 wk after the procedures*

	4 Weeks		5 Weeks		6 Weeks	
	Control group	ANS group	Control group	ANS group	Control group	ANS group
Number of mice/group	5	5	12	12	12	11
LV end-diastolic dimension, mm	3.5 ± 0.20	3.4 ± 0.24	3.6 ± 0.18	3.5 ± 0.45	3.6 ± 0.24	4.0 ± 0.48*
LV fractional shortening, %	38 ± 5	37 ± 9	42 ± 4	36 ± 6*	39 ± 3	26 ± 9†
LV weight/tibial length, mg/mm	4.35 ± 0.58	6.80 ± 0.69†	4.53 ± 0.40	8.03 ± 1.29†	4.59 ± 0.36	8.90 ± 1.22†
Lung weight/tibial length, mg/mm	7.35 ± 0.71	7.33 ± 0.66	7.47 ± 0.56	9.36 ± 2.77*	7.12 ± 0.40	10.00 ± 3.11†
Mice with congestive heart failure	0	0	0	3 of 12 (25%)	0	7 of 11 (73%)

Results are means ± SD. LV, left ventricular. Congestive heart failure was defined as lung weight/tibial length greater than control +2 ± SD. *$P < 0.05$ vs. the control group; †$P < 0.01$ vs. the control group.

II pathway in the heart is also thought to be one of the crucial factors in the development of chronic HF from the results of many clinical trials and experiments (27). CKD is an independent risk factor in chronic HF. Uninephrectomy induces renal dysfunction, especially under the high-salt condition, in animal models (2, 38), although it is controversial whether uninephrectomy itself is at a risk factor for CKD in humans from the results of patients with cortical tumors (16, 47). Although it is unclear in patients, in the mouse model of this study, uninephrectomy in the presence of hypertension and/or salt loading induced renal dysfunction, which is one of the key determinants in the development of HF in patients with hypertension (27). Thus, the mouse model of the present study is thought to at least partially mimic renal dysfunction, which is one of the key features of HHD in patients.

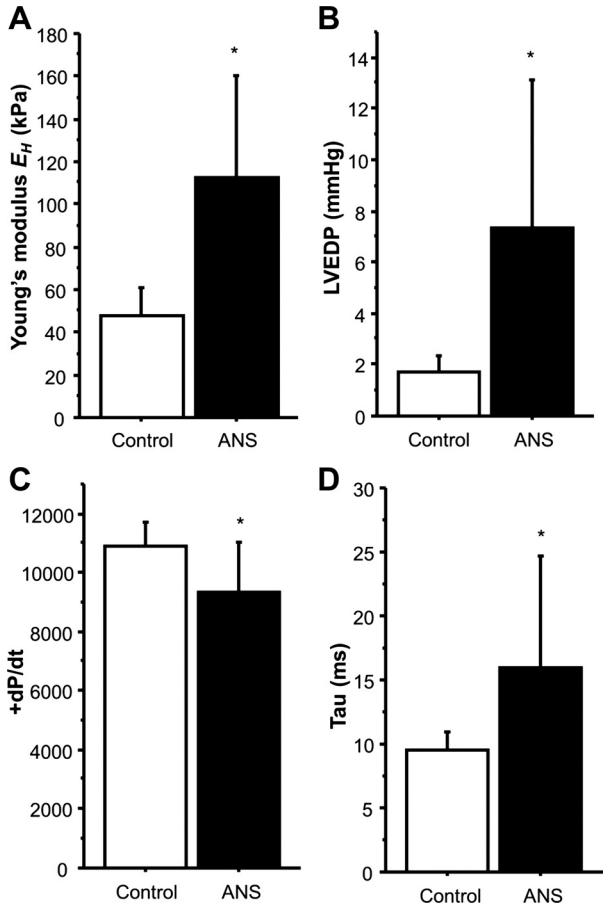

Fig. 4. Myocardial stiffness and hemodynamic parameters. *A*: Young's modulus (E_H), an index of LV myocardial stiffness, in control and ANS mice at 4 wk after surgery. *B–D*: LV end-diastolic pressure (LVEDP; *B*), maximum rate of LV pressure development (+dP/d*t*; *C*), time constant of LV relaxation (τ; *D*) in control and ANS mice at 6 wk after surgery.

Mouse HF models have the great benefit of the wide availability of transgenic or knockout strains of a gene of interest to clarify the pathogenesis of HF and identify novel therapeutic targets (35). The TAC mouse model is a pressure overload model and has been used as a mouse HF model in a number of studies. TAC induces acute significant pressure overload just after the operation and does not necessarily mimic the clinical time course of HHD. Gradual pressure overload models have been reported (43), but it has proven difficult to establish such models in mice. TAC also promotes high mortality, especially just after the operation (26, 28). The performance of TAC in mice requires great surgical expertise, and it might induce a variety of loading conditions and phenotypes of mice (28). Variability in the model affects the sample size required to detect the effects of genetic or pharmacological interventions. The procedure for creating the ANS model in the present study is relatively easier compared with the TAC model, and we can place constant load on each mouse in this model. Approximately one-third of ANS mice died between 3 to 6 wk after the procedures, mainly due to HF, and the rest of the ANS mice showed a significant increase in lung weight at 5–6 wk after procedures. These phenotypes of ANS mice were highly reproducible, and early or perioperative death was rare in this model. Thus, it is suggested that the ANS mouse model has a high incidence of HF with simple and stable experimental procedures.

Previous studies have shown that C57BL/6 mice infused with ANG II show either normal (10, 12, 49) or only minimal impairment in LV systolic function (53) and do not demonstrate HF. In the present study, by adding both high salt intake and unilateral nephrectomy to ANG II infusion, cardiac function of ANS mice was significantly impaired, and mice devel-

Table 4. *Reproducibility of phenotypes of ANS model mice*

	Experiment 1	Experiment 2	Experiment 3
Operated mice	5	5	7
Mortality	1 of 5 (20%)	2 of 5 (40%)	3 of 7 (42%)
Surviving mice	4	3	4
Mice with congestive heart failure	3 of 4 (75%)	2 of 3 (67%)	3 of 4 (75%)
LV weight/tibial length, mg/mm	9.43 ± 1.12	9.01 ± 1.51	8.29 ± 1.14

Results are means ± SD. Congestive heart failure was defined as lung weight/tibial length greater than control +2 ± SD.

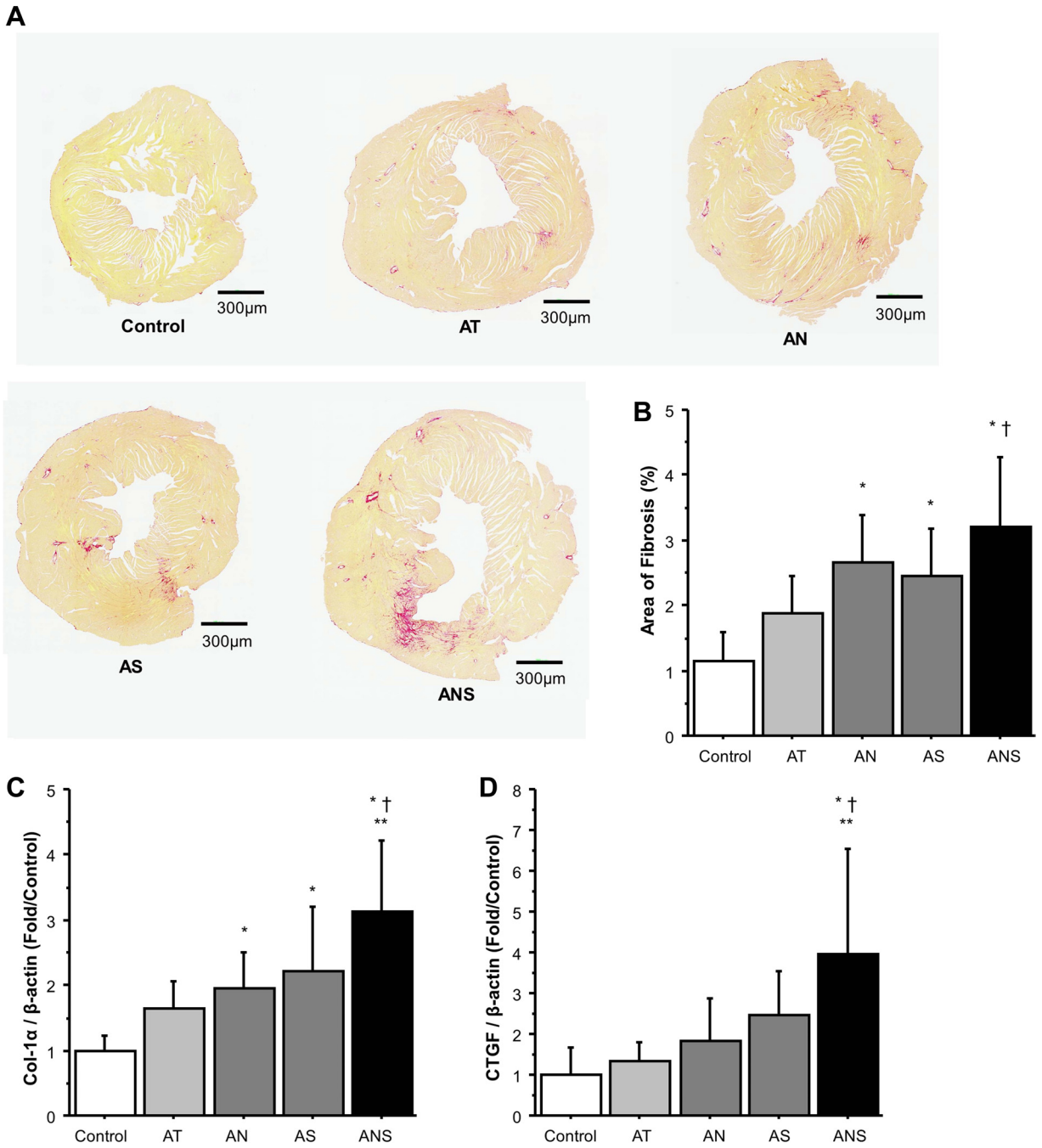

Fig. 5. LV fibrosis in the mouse model. *A*: typical Sirius Red staining of the LV in each group. *B*: percent area of LV fibrosis in control, AT, AN, AS, and ANS mice. *C* and *D*: collagen type 1α (Col-1α; *C*) and connective tissue growth factor (CTGF; *D*) gene expression in the LVs of the five groups. *$P < 0.05$ vs. the control group; †$P < 0.05$ vs. the AT group; **$P < 0.05$ vs. the AN group.

oped HF without a further elevation of blood pressure. Similar cardiomyocyte hypertrophy was seen in the LVs of mice with ANG II infusion irrespective of high salt intake or unilateral nephrectomy. Thus, the enhanced pressure overload and hypertrophy of cardiomyocytes are not considered as the main causes of overt HF in ANS mice.

We preliminary tested the phenotypes in mice with several doses of ANG II infusion, uninephrectomy, and salt loading (data not shown), which demonstrated that 1.2 $mg \cdot kg^{-1} \cdot day^{-1}$ of ANG II infusion is an adequate dose to induce HF in this mouse model of HHD. LV myocardial stiffness increased, LV diastolic and systolic function (as assessed by LV catheterization) was impaired, and LVEDP was elevated with pulmonary edema in ANS mice. LV myocardial stiffening is a major determinant of LV diastolic dysfunction, and it is thought to be provoked by LV fibrosis (51). There might be a mechanism demonstrating that Na^+ and volume overload in the heart with LV diastolic and systolic dysfunction induce overt HF in ANS mice. In the present study, LV ANP mRNA levels increased in AN mice and further increased in ANS mice. LV BNP mRNA

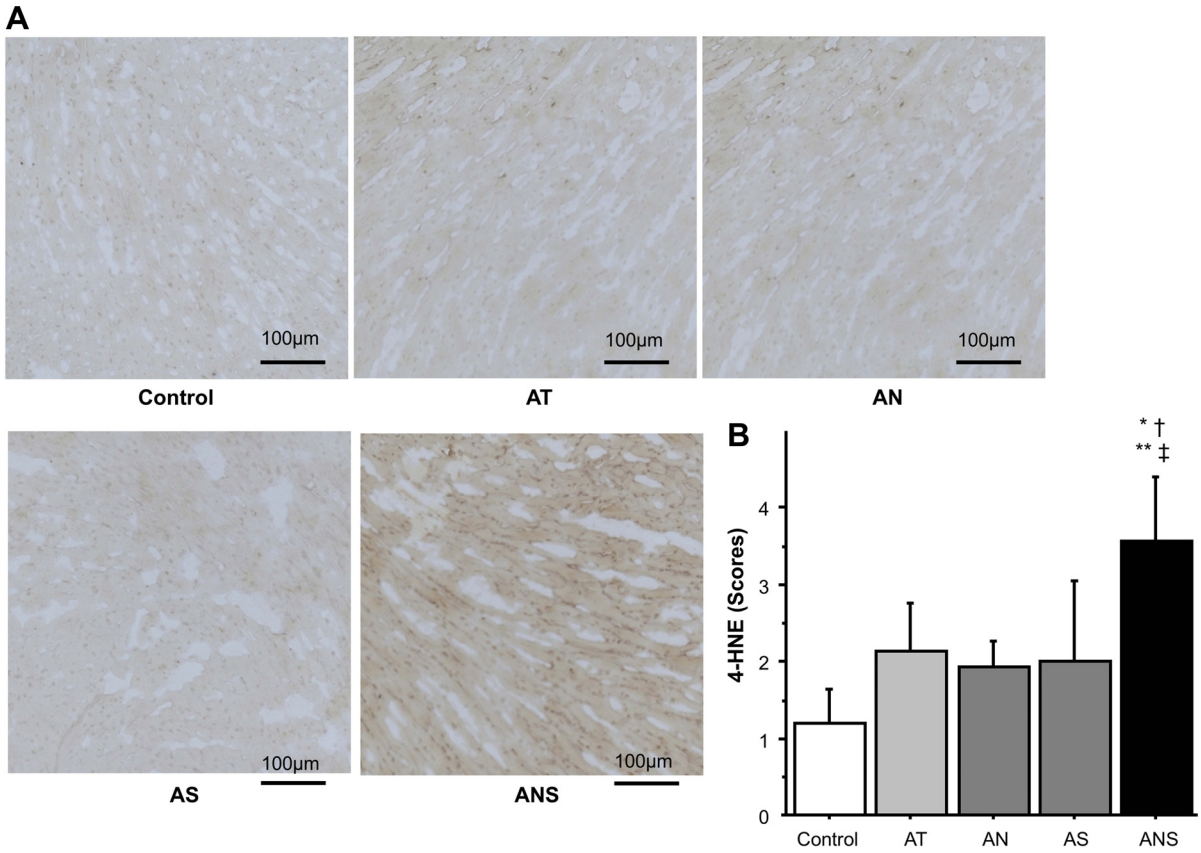

Fig. 6. Oxidative stress in mouse LVs. *A*: typical 4-hydroxy-2-nonenal (4-HNE) staining of the LVs of each group. *B*: scores for semiquantification of 4-HNE staining in the LVs of control, AT, AN, AS, and ANS mice. Values are means ± SD of data from 7–9 mice/group. *$P < 0.05$ vs. the control group; †$P < 0.05$ vs. the AT group; **$P < 0.05$ vs. the AN group; ‡$P < 0.05$ vs. the AS group.

levels did not significantly change in AN mice but increased in AS and ANS mice. This suggests that LV ANP expression reflected both cardiac hypertrophy and the salt loading condition, but BNP expression was associated with the salt loading condition and LV fibrosis in our mouse model. These results are consistent with our previous report (39), which showed that ventricular BNP expression was closely related with LV fibrosis in the rat model of diastolic HF. Renal dysfunction has been shown in mice with ANG II infusion and nephrectomy, but overt HF was observed only in ANS mice. When salt intake is increased, Na^+ excretion is promoted, and this increases the glomerular filtration rate and reduces tubular Na^+ reabsorption in normal renal function (18). It has been reported that uninephrectomy does not affect Na^+ excretion under basal conditions but that uninephrectomy induces salt sensitivity and renal injury in the rat model after increased Na^+ intake (2, 38).

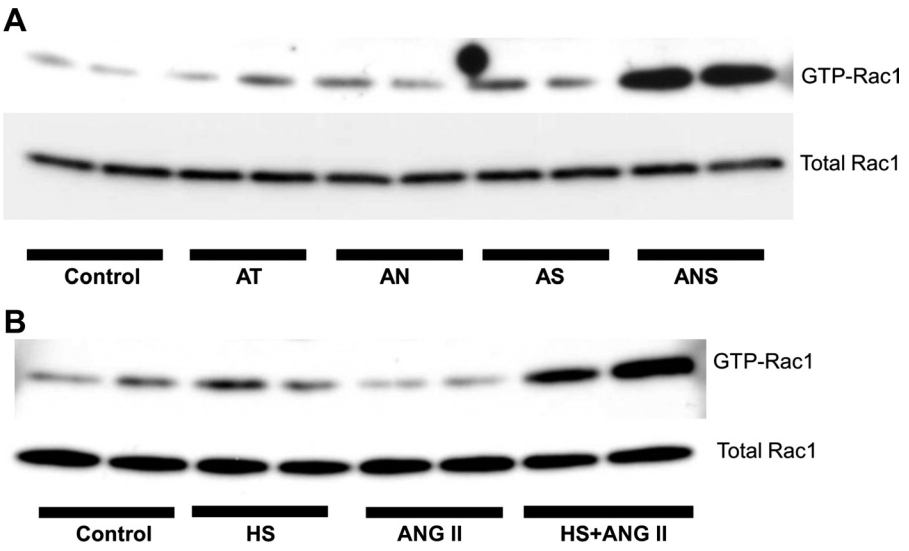

Fig. 7. Rac1 activity in the LVs of the mouse model and cultured cardiomyocytes. *A*: representative Western blots of GTP-bound active Rac1 (GTP-Rac1) and total Rac1 in the LVs of control, AT, AN, AS, and ANS mice. *B*: representative examples of expression of GTP-bound Rac1 and total Rac1 in rat neonatal cardiomyocytes treated with control medium (150 mmol/l Na^+), high-salt (HS) medium (162 mmol/l Na^+), ANG II (1 μmol/l), or both high-salt medium and ANG II for 3 h.

Compensatory mechanisms against Na^+ loading might be insufficient because of renal dysfunction in ANS mice. ANG II can also increase tubular Na^+ reabsorption (22). Thus, ANG II infusion and renal dysfunction induced an impairment of Na^+ homeostasis in ANS mice, and ANS mice are considered to have a tendency toward Na^+ and volume retention. This might be one of the mechanisms that allow ANS mice to demonstrate overt HF. The CKD mouse model induced by 5/6th nephrectomy has also been reported to manifest the HF phenotype, but this has shown conflicting results regarding a cardiac phenotype, such as systolic dysfunction or HF, because the technical instability of 5/6th nephrectomy does not allow the reproduction of similar renal dysfunction in each mouse (20, 23, 24).

It has been reported that Rac1 is activated by high salt loading in the kidney of rodent models of salt-sensitive hypertension and plays a key role in salt sensitivity and salt-induced hypertension (42). Our study suggests that Rac1 activity in cultured cardiomyocytes was increased when cardiomyocytes were in the high Na^+ condition and stimulated with ANG II. In vivo, Rac1 activity was enhanced only in the hearts of ANS mice. It has been reported that Rac1 promotes ROS generation in the heart of the mouse TAC model (3), doxorubicin-induced cardiac toxicity (52), and diabetic cardiomyopathy (41). Previous clinical and experimental studies (1, 14) have provided substantial evidence showing that oxidative stress is enhanced in HF. Excessive ROS production can lead to irreversible cell damage and death in the myocardium, which can impair LV contractile function (8, 48). ROS also stimulate cardiac fibroblast proliferation and activate matrix metalloproteinases, leading to remodeling of the extracellular matrix (40, 48). Rac1 might play a role in LV fibrosis and LV systolic dysfunction through ROS production and contribute to the development of HF in ANS mice.

In conclusion, mice treated with high salt loading, nephrectomy, and ANG II infusion demonstrated a high incidence of HF with simple experimental procedures and reproducible phenotypes. This mouse model will be of interest in investigations of the pathophysiology of HF in HHD and in establishing new options for therapy for HF.

ACKNOWLEDGMENTS

The authors are grateful to Saori Nanbu for the excellent technical assistance in the experiments.

DISCLOSURES

No conflicts of interest, financial or otherwise, are declared by the author(s).

AUTHOR CONTRIBUTIONS

Author contributions: Y. Tsukamoto, T. Mano, Y. Sakata, T.O., Y. Takeda, S.T., Y.O., Y.I., Y. Saito, T. Miwa, K.Y., and I.K. conception and design of research; Y. Tsukamoto, S.T., Y.O., Y.I., Y. Saito, R.I., and M.H. performed experiments; Y. Tsukamoto, T. Mano, Y. Sakata, T.O., Y. Takeda, S.T., Y.O., Y.I., Y. Saito, R.I., M.H., M.K., and T. Miwa analyzed data; Y. Tsukamoto, T. Mano, Y. Sakata, T.O., Y. Takeda, S.T., Y.O., Y.I., Y. Saito, R.I., M.H., M.K., T. Miwa, K.Y., and I.K. interpreted results of experiments; Y. Tsukamoto, T. Mano, and M.K. prepared figures; Y. Tsukamoto, T. Mano, M.H., and M.K. drafted manuscript; Y. Tsukamoto, T. Mano, Y. Sakata, T.O., Y. Takeda, T. Miwa, K.Y., and I.K. edited and revised manuscript; Y. Tsukamoto, T. Mano, Y. Sakata, T.O., Y. Takeda, S.T., Y.O., Y.I., Y. Saito, R.I., M.H., M.K., T. Miwa, K.Y., and I.K. approved final version of manuscript.

REFERENCES

1. **Belch JJ, Bridges AB, Scott N, Chopra M.** Oxygen free radicals and congestive heart failure. *Br Heart J* 65: 245–248, 1991.
2. **Carlstrom M, Sallstrom J, Skott O, Larsson E, Persson AE.** Unilephrectomy in young age or chronic salt loading causes salt-sensitive hypertension in adult rats. *Hypertension* 49: 1342–1350, 2007.
3. **Custodis F, Eberl M, Kilter H, Böhm M, Laufs U.** Association of RhoGDIα with Rac1 GTPase mediates free radical production during myocardial hypertrophy. *Cardiovasc Res* 71: 342–351, 2006.
4. **Doi R, Masuyama T, Yamamoto K, Doi Y, Mano T, Sakata Y, Ono K, Kuzuya T, Hirota S, Koyama T, Miwa T, Hori M.** Development of different phenotypes of hypertensive heart failure: systolic versus diastolic failure in Dahl salt-sensitive rats. *J Hypertens* 18: 111–120, 2000.
5. **Ellmers LJ, Knowles JW, Kim HS, Smithies O, Maeda N, Cameron VA.** Ventricular expression of natriuretic peptides in $Npr1^{-/-}$ mice with cardiac hypertrophy and fibrosis. *Am J Physiol Heart Circ Physiol* 283: H707–H714, 2002.
6. **Go AS, Chertow GM, Fan D, McCulloch CE, Hsu CY.** Chronic kidney disease and the risks of death, cardiovascular events, and hospitalization. *N Engl J Med* 351: 1296–1305, 2004.
7. **Graudal NA, Galløe AM, Garred P.** Effects of sodium restriction on blood pressure, renin, aldosterone, catecholamines, cholesterols, and triglyceride: a meta-analysis. *JAMA* 279: 1383–1391, 1998.
8. **Grieve DJ, Shah AM.** Oxidative stress in heart failure. More than just damage. *Eur Heart J* 24: 2161–2163, 2003.
9. **Gu JW, Anand V, Shek EW, Moore MC, Brady AL, Kelly WC, Adair TH.** Sodium induces hypertrophy of cultured myocardial myoblasts and vascular smooth muscle cells. *Hypertension* 31: 1083–1087, 1998.
10. **Harding P, Yang XP, He Q, Lapointe MC.** Lack of microsomal prostaglandin E synthase-1 reduces cardiac function following angiotensin II infusion. *Am J Physiol Heart Circ Physiol* 300: H1053–H1061, 2011.
11. **Hart CY, Meyer DM, Tazelaar HD, Grande JP, Burnett JC, Housmans PR, Redfield MM.** Load versus humoral activation in the genesis of early hypertensive heart disease. *Circulation* 104: 215–220, 2001.
12. **Haudek SB, Cheng J, Du J, Wang Y, Hermosillo-Rodriguez J, Trial J, Taffet GE, Entman ML.** Monocytic fibroblast precursors mediate fibrosis in angiotensin-II-induced cardiac hypertrophy. *J Mol Cell Cardiol* 49: 499–507, 2010.
13. **Hikoso S, Yamaguchi O, Nakano Y, Takeda T, Omiya S, Mizote I, Taneike M, Oka T, Tamai T, Oyabu J, Uno Y, Matsumura Y, Nishida K, Suzuki K, Kogo M, Hori M, Otsu K.** The IκB kinase β/nuclear factor κB signaling pathway protects the heart from hemodynamic stress mediated by the regulation of manganese superoxide dismutase expression. *Circ Res* 105: 70–79, 2009.
14. **Hill MF, Singal PK.** Antioxidant and oxidative stress changes during heart failure subsequent to myocardial infarction in rats. *Am J Pathol* 148: 291–300, 1996.
15. **Houser SR, Margulies KB, Murphy AM, Spinale FG, Francis GS, Prabhu SD, Rockman HA, Kass DA, Molkentin JD, Sussman MA, Koch WJ, Koch W; American Heart Association Council on Basic Cardiovascular Sciences, Council on Clinical Cardiology, Council on Functional Genomics and Translational Biology**. Animal models of heart failure: a scientific statement from the American Heart Association. *Circ Res* 111: 131–150, 2012.
16. **Huang WC, Levey AS, Serio AM, Snyder M, Vickers AJ, Raj GV, Scardino PT, Russo P.** Chronic kidney disease after nephrectomy in patients with renal cortical tumours: a retrospective cohort study. *Lancet Oncol* 7: 735–740, 2006.
17. **Ishii R, Higashimori M, Tadakuma K, Kaneko M, Tamaki S, Sakata Y, Yamamoto K.** Balloon type elasticity sensing for left ventricle of small laboratory animal. *Conf Proc IEEE Eng Med Biol Soc* 2011: 904–907, 2011.
18. **Ito S, Nagasawa T, Abe M, Mori T.** Strain vessel hypothesis: a viewpoint for linkage of albuminuria and cerebro-cardiovascular risk. *Hypertens Res* 32: 115–121, 2009.
19. **Kakoki M, Kizer CM, Yi X, Takahashi N, Kim HS, Bagnell CR, Edgell CJ, Maeda N, Jennette JC, Smithies O.** Senescence-associated phenotypes in Akita diabetic mice are enhanced by absence of bradykinin B_2 receptors. *J Clin Invest* 116: 1302–1309, 2006.
20. **Kennedy DJ, Elkareh J, Shidyak A, Shapiro AP, Smaili S, Mutgi K, Gupta S, Tian J, Morgan E, Khouri S, Cooper CJ, Periyasamy SM, Xie Z, Malhotra D, Fedorova OV, Bagrov AY, Shapiro JI.** Partial nephrectomy as a model for uremic cardiomyopathy in the mouse. *Am J Physiol Renal Physiol* 294: F450–F454, 2008.
21. **Keppler A, Gretz N, Schmidt R, Kloetzer HM, Groene HJ, Lelongt B, Meyer M, Sadick M, Pill J.** Plasma creatinine determination in mice and

rats: an enzymatic method compares favorably with a high-performance liquid chromatography assay. *Kidney Int* 71: 74–78, 2007.
22. **Kopkan L, Cervenka L.** Renal interactions of renin-angiotensin system, nitric oxide and superoxide anion: implications in the pathophysiology of salt-sensitivity and hypertension. *Physiol Res* 58, *Suppl* 2: S55–S67, 2009.
23. **Leelahavanichkul A, Yan Q, Hu X, Eisner C, Huang Y, Chen R, Mizel D, Zhou H, Wright EC, Kopp JB, Schnermann J, Yuen PS, Star RA.** Angiotensin II overcomes strain-dependent resistance of rapid CKD progression in a new remnant kidney mouse model. *Kidney Int* 78: 1136–1153, 2010.
24. **Li Y, Takemura G, Okada H, Miyata S, Maruyama R, Esaki M, Kanamori H, Li L, Ogino A, Ohno T, Kondo T, Nakagawa M, Minatoguchi S, Fujiwara T, Fujiwara H.** Molecular signaling mediated by angiotensin II type 1A receptor blockade leading to attenuation of renal dysfunction-associated heart failure. *J Card Fail* 13: 155–162, 2007.
25. **Liao CH, Akazawa H, Tamagawa M, Ito K, Yasuda N, Kudo Y, Yamamoto R, Ozasa Y, Fujimoto M, Wang P, Nakauchi H, Nakaya H, Komuro I.** Cardiac mast cells cause atrial fibrillation through PDGF-A-mediated fibrosis in pressure-overloaded mouse hearts. *J Clin Invest* 120: 242–253, 2010.
26. **Liao Y, Ishikura F, Beppu S, Asakura M, Takashima S, Asanuma H, Sanada S, Kim J, Ogita H, Kuzuya T, Node K, Kitakaze M, Hori M.** Echocardiographic assessment of LV hypertrophy and function in aortic-banded mice: necropsy validation. *Am J Physiol Heart Circ Physiol* 282: H1703–H1708, 2002.
27. **Luque M, de Rivas B, Divison JA, Marquez E, Sobreviela E.** Relationship between renal function and heart failure in hypertensive patients. *Intern Med J* 40: 76–79, 2010.
28. **Mohammed SF, Storlie JR, Oehler EA, Bowen LA, Korinek J, Lam CS, Simari RD, Burnett JC Jr, Redfield MM.** Variable phenotype in murine transverse aortic constriction. *Cardiovasc Pathol* 21: 188–198, 2012.
29. **Ohtani T, Mano T, Hikoso S, Sakata Y, Nishio M, Takeda Y, Otsu K, Miwa T, Masuyama T, Hori M, Yamamoto K.** Cardiac steroidogenesis and glucocorticoid in the development of cardiac hypertrophy during the progression to heart failure. *J Hypertens* 27: 1074–1083, 2009.
30. **Ohtani T, Ohta M, Yamamoto K, Mano T, Sakata Y, Nishio M, Takeda Y, Yoshida J, Miwa T, Okamoto M, Masuyama T, Nonaka Y, Hori M.** Elevated cardiac tissue level of aldosterone and mineralocorticoid receptor in diastolic heart failure: beneficial effects of mineralocorticoid receptor blocker. *Am J Physiol Regul Integr Comp Physiol* 292: R946–R954, 2007.
31. **Oka T, Maillet M, Watt AJ, Schwartz RJ, Aronow BJ, Duncan SA, Molkentin JD.** Cardiac-specific deletion of Gata4 reveals its requirement for hypertrophy, compensation, and myocyte viability. *Circ Res* 98: 837–845, 2006.
32. **Omiya S, Hikoso S, Imanishi Y, Saito A, Yamaguchi O, Takeda T, Mizote I, Oka T, Taneike M, Nakano Y, Matsumura Y, Nishida K, Sawa Y, Hori M, Otsu K.** Downregulation of ferritin heavy chain increases labile iron pool, oxidative stress and cell death in cardiomyocytes. *J Mol Cell Cardiol* 46: 59–66, 2009.
33. **Omori Y, Ohtani T, Sakata Y, Mano T, Takeda Y, Tamaki S, Tsukamoto Y, Kamimura D, Aizawa Y, Miwa T, Komuro I, Soga T, Yamamoto K.** L-Carnitine prevents the development of ventricular fibrosis and heart failure with preserved ejection fraction in hypertensive heart disease. *J Hypertens* 30: 1834–1844, 2012.
34. **Pacher P, Nagayama T, Mukhopadhyay P, Bátkai S, Kass DA.** Measurement of cardiac function using pressure-volume conductance catheter technique in mice and rats. *Nat Protoc* 3: 1422–1434, 2008.
35. **Patten RD, Hall-Porter MR.** Small animal models of heart failure: development of novel therapies, past and present. *Circ Heart Fail* 2: 138–144, 2009.
36. **Pfeffer JM, Pfeffer MA, Mirsky I, Braunwald E.** Regression of left ventricular hypertrophy and prevention of left ventricular dysfunction by captopril in the spontaneously hypertensive rat. *Proc Natl Acad Sci USA* 79: 3310–3314, 1982.
37. **Querejeta R, Lopez B, Gonzalez A, Sanchez E, Larman M, Martinez Ubago JL, Diez J.** Increased collagen type I synthesis in patients with heart failure of hypertensive origin: relation to myocardial fibrosis. *Circulation* 110: 1263–1268, 2004.
38. **Rodriguez-Gomez I, Wangensteen R, Perez-Abud R, Quesada A, Del Moral RG, Osuna A, O'Valle F, de Dios Luna J, Vargas F.** Long-term consequences of uninephrectomy in male and female rats. *Hypertension* 60: 1458–1463, 2012.
39. **Sakata Y, Yamamoto K, Masuyama T, Mano T, Nishikawa N, Kuzuya T, Miwa T, Hori M.** Ventricular production of natriuretic peptides and ventricular structural remodeling in hypertensive heart failure. *J Hypertens* 19: 1905–1912, 2001.
40. **Segura AM, Frazier OH, Buja LM.** Fibrosis and heart failure. *Heart Fail Rev.* In press.
41. **Shen E, Li Y, Shan L, Zhu H, Feng Q, Arnold JM, Peng T.** Rac1 is required for cardiomyocyte apoptosis during hyperglycemia. *Diabetes* 58: 2386–2395, 2009.
42. **Shibata S, Mu S, Kawarazaki H, Muraoka K, Ishizawa K, Yoshida S, Kawarazaki W, Takeuchi M, Ayuzawa N, Miyoshi J, Takai Y, Ishikawa A, Shimosawa T, Ando K, Nagase M, Fujita T.** Rac1 GTPase in rodent kidneys is essential for salt-sensitive hypertension via a mineralocorticoid receptor-dependent pathway. *J Clin Invest* 121: 3233–3243, 2011.
43. **Siri FM, Nordin C, Factor SM, Sonnenblick E, Aronson R.** Compensatory hypertrophy and failure in gradual pressure-overloaded guinea pig heart. *Am J Physiol Heart Circ Physiol* 257: H1016–H1024, 1989.
44. **Strazzullo P, D'Elia L, Kandala NB, Cappuccio FP.** Salt intake, stroke, and cardiovascular disease: meta-analysis of prospective studies. *BMJ* 339: b4567, 2009.
45. **Tamaki S, Mano T, Sakata Y, Ohtani T, Takeda Y, Kamimura D, Omori Y, Tsukamoto Y, Ikeya Y, Kawai M, Kumanogoh A, Hagihara K, Ishii R, Higashimori M, Kaneko M, Hasuwa H, Miwa T, Yamamoto K, Komuro I.** Interleukin-16 promotes cardiac fibrosis and myocardial stiffening in heart failure with preserved ejection fraction. *PLos One* 8: e68893, 2013.
46. **Terui T, Shimamoto Y, Yamane M, Kobirumaki F, Ohtsuki I, Ishiwata S, Kurihara S, Fukuda N.** Regulatory mechanism of length-dependent activation in skinned porcine ventricular muscle: role of thin filament cooperative activation in the Frank-Starling relation. *J Gen Physiol* 136: 469–482, 2010.
47. **Torricelli FC, Danilovic A, Marchini GS, Sant'Anna AC, Dall'Oglio MF, Srougi M.** Can we predict which patients will evolve to chronic kidney disease after nephrectomy for cortical renal tumors? *Int Braz J Urol* 38: 637–644, 2012.
48. **Tsutsui H, Kinugawa S, Matsushima S.** Oxidative stress and heart failure. *Am J Physiol Heart Circ Physiol* 301: H2181–H2190, 2011.
49. **Xu Z, Okamoto H, Akino M, Onozuka H, Matsui Y, Tsutsui H.** Pravastatin attenuates left ventricular remodeling and diastolic dysfunction in angiotensin II-induced hypertensive mice. *J Cardiovasc Pharmacol* 51: 62–70, 2008.
50. **Yamamoto K, Masuyama T, Sakata Y, Doi R, Ono K, Mano T, Kondo H, Kuzuya T, Miwa T, Hori M.** Local neurohumoral regulation in the transition to isolated diastolic heart failure in hypertensive heart disease: absence of AT_1 receptor downregulation and 'overdrive' of the endothelin system. *Cardiovasc Res* 46: 421–432, 2000.
51. **Yamamoto K, Masuyama T, Sakata Y, Nishikawa N, Mano T, Yoshida J, Miwa T, Sugawara M, Yamaguchi Y, Ookawara T, Suzuki K, Hori M.** Myocardial stiffness is determined by ventricular fibrosis, but not by compensatory or excessive hypertrophy in hypertensive heart. *Cardiovasc Res* 55: 76–82, 2002.
52. **Yoshida M, Shiojima I, Ikeda H, Komuro I.** Chronic doxorubicin cardiotoxicity is mediated by oxidative DNA damage-ATM-p53-apoptosis pathway and attenuated by pitavastatin through the inhibition of Rac1 activity. *J Mol Cell Cardiol* 47: 698–705, 2009.
53. **Zhang R, Zhang YY, Huang XR, Wu Y, Chung AC, Wu EX, Szalai AJ, Wong BC, Lau CP, Lan HY.** C-reactive protein promotes cardiac fibrosis and inflammation in angiotensin II-induced hypertensive cardiac disease. *Hypertension* 55: 953–960, 2010.